

CONTRAST MANIPULATION AND CONTROLLABLE SPATIAL FILTERING VIA PHOTOREFRACTIVE TWO-BEAM COUPLING

J.A. KHOURY, G. HUSSAIN¹ and R.W. EASON¹
Department of Physics, University of Essex, Colchester CO4 3SQ, UK

Received 9 September 1988; revised manuscript received 6 December 1988

A scheme is presented that achieves passive controllable spatial filtering via two-beam coupling in BaTiO₃, between a reference beam and the optical Fourier transform of an input image. The nature of the spatial filtering is determined by the intensity dependent gain seen by each component of the Fourier transform. By appropriate choice of intensity ratio, the operations of contrast enhancement, feature extraction, and defect enhancement are possible, and representative examples of these are given.

1. Introduction

Spatial filtering, which relies on the insertion of masks, slits or other objects such as stops in the Fourier transform plane of an optical imaging system, is a well established technique for optical image processing. By restricting the range of spatial frequency components of an object that are available for subsequent image formation, a variety of filtering operations is possible such as smoothing or directional filtering. These established or conventional methods, however, suffer from two serious drawbacks. Firstly, the possibility of updating or renewing these Fourier masks at the speeds required for real-time processing at, for example, TV frame rates, is extremely limited. Secondly the filtering operation is of necessity one of *reducing* the amplitude of some of the spectral components, while leaving others unchanged: there is no possibility of *enhancing* some spectral features at the expense of others.

Recently, however, photorefractive materials have been used for a range of optical data processing applications such as spatial filtering [1], edge enhancement [2-4], and defect analysis in periodic objects [5]. These non-linear crystalline materials, of which perhaps Bismuth Silicon Oxide (BSO) and BaTiO₃ are most commonly used, allow a new approach to

real-time Fourier modification techniques. While degenerate four-wave mixing (DFWM) is perhaps the most versatile technique for the applications above, the DFWM arrangement typically has the characteristic of reduction of certain frequencies rather than any enhancement. For the specific case of contrast enhancement the requirement is for partial or variable suppression of the DC term in the object's Fourier transform.

In this paper we demonstrate contrast enhancement that relies on two beam coupling in photorefractive BaTiO₃ in which the large electro-optic coefficient allows Fourier plane modification via variable optical gain, thereby opening up possibilities of simultaneous contrast enhancement and an increase in brightness.

2. Theory

Fig. 1 shows the standard configuration for two-beam coupling experiments in which two mutually coherent beams intersect at a crossing angle θ within the photorefractive medium of length L . The direction of energy transfer between the two beams depends on the crystal orientation and sign of the photoinduced charge carriers, whereas the magnitude of the coupling depends on materials parameters such as trap density and effective electro-optic coefficient, and hence on the experimental geometry via angles

¹ Now at Department of Physics, Southampton University, Highfield, Southampton SO9 5NH, UK.

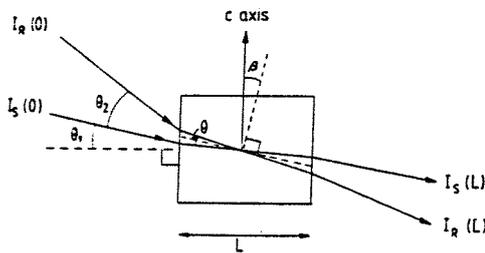


Fig. 1. Geometry for reference and signal beams inside BaTiO₃.

θ and β [6]. In fig. 1, energy is coupled from the reference beam I_R into the signal beam I_S .

The gain, G , experienced by the signal beam I_S in this case can be deduced from consideration of the relevant coupled wave equations [7]. The solution is given by the following equation

$$G = \frac{I_S(L)}{I_S(0)} = \frac{(1+r) \exp(\Gamma L_{\text{eff}})}{1+r \exp(\Gamma L_{\text{eff}})}, \quad (1)$$

in which r is the beam intensity ratio $I_S(0)/I_R(0)$ as shown in fig. 1. Γ is the two beam coupling gain coefficient [8], and L_{eff} is the effective interaction length. Eq. (1) is valid only in the strictly lossless case. To account for absorption and reflection losses it is experimentally convenient to measure the gain G as the ratio of $I_S(L)$ with, and without, the presence of $I_R(0)$.

Fig. 2 shows the measured plot of G versus r for the geometry used. For $r \approx 1$, the gain is necessarily small, approaching a limiting value (in the lossless case) of 2 for $\Gamma L_{\text{eff}} \gg 1$. On the other hand, for $r \ll 1$, eq. (1) reduces to a saturated value of G equal to G_{sat} , given by

$$G_{\text{sat}} = \exp(\Gamma L_{\text{eff}}). \quad (2)$$

For intermediate values of r , there is the experimentally interesting region where $G \propto 1/r$, and there exists the possibility for observing transfer characteristics for I_S which show, for example, optical limiting. It is this latter region that we are considering in this paper.

Fig. 3 shows the experimental arrangement in which two beam coupling occurs between a reference beam I_R , and a signal beam I_S that is the Fourier transform of an object, formed in the back focal plane of lens L , placed one focal length from the BaTiO₃ crystal. The gain G that is observed in the image plane

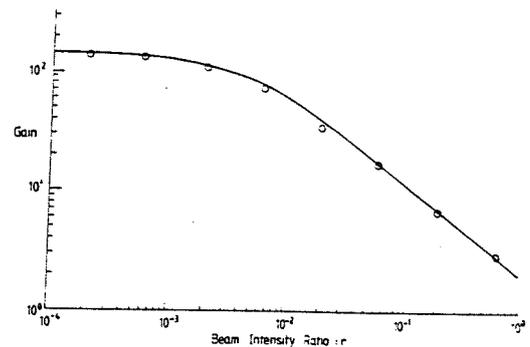


Fig. 2. Plot of gain, G , versus beam intensity ratio r , defined as $I_S(0)/I_R(0)$, for the geometry of fig. 1. The dots are experimental points and the solid curve is calculated according to eq. (1) using a value of $\Gamma L_{\text{eff}} = 5 \text{ cm}^{-1}$. The data has been superimposed to achieve a visual best fit, as different spot sizes for references and signal beams produce an uncertainty in estimating an absolute value for r .

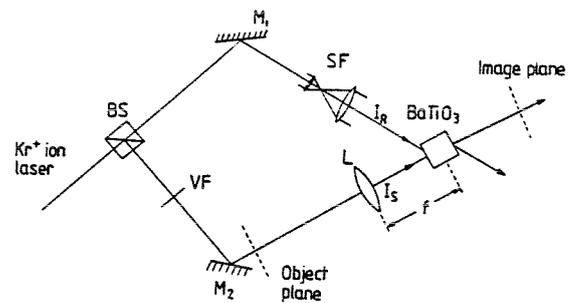


Fig. 3. Experimental arrangement for contrast manipulation.

will depend therefore on the respective intensity ratios within the spatial frequency distribution in the transform plane, according to eq. (1). It is clear, therefore, that a method exists here for performing spatial filtering operations whose character depends on the operating point set via r .

This idea has been recognised before, and edge enhancement using this method has already been demonstrated by Fainman et al. [6], in which the high spatial frequencies of an object have experienced higher gain compared to the lower frequencies, due to their respective intensities. For the work reported in ref. [6], however, which investigated uniform image amplification, this was considered detrimental, and further studies were not reported.

We are extending this possibility here to explicitly consider several operations which rely on just this characteristic. We examine here contrast enhance-

ment which requires preferential amplification of all spatial frequencies compared to the dc term, and also feature extraction and defect enhancement which similarly require controllable and non-linear amplification of the higher spatial frequencies present in an object.

For contrast enhancement we may consider an object with a high initial background illumination, whose spatial transmission $f(x, y)$ is given by

$$f(x, y) = A_0 + g(x, y) \quad (3)$$

where A_0 is a uniform (high) background level.

The Fourier transform of $f(x, y)$ is given by

$$F(\nu_x, \nu_y) = A_0\delta(0) + G(\nu_x, \nu_y) \quad (4)$$

Merely removing some part of the dc term $A_0\delta(0)$ in eq. (4) is not sufficient as this also removes overall illumination or image brightness, a problem referred to earlier. Using non-linear coupling in BaTiO_3 , however, we can initially set the operating point on the G versus r curve shown in fig. 2, so that the dc term experiences unity gain, while the features represented by $G(\nu_x, \nu_y)$ achieve considerable gain $\gg 1$. This removes the former problem of increasing contrast at the expense of overall illumination.

The possibility also exists for selectively amplifying any particular range of spatial frequencies to examine whether an object contains a specific feature, or looking at an input and selectively amplifying spatial frequency dependent defects, for example dust particles or scratches. We shall give examples of our results for these two latter cases as well as those for contrast enhancement in the following section.

3. Experimental and results

The experimental arrangement is shown in fig. 3, and is essentially the standard configuration for two beam coupling. The laser used was a Kr^+ ion laser operating at $\lambda = 530.9$ nm in multilongitudinal mode. Beam splitter BS divides the input into two beams with an approximate 50/50 split. The transmitted beam was expanded to a diameter of ≈ 4 mm via the spatial filter/beam expander combination SF, and entered the crystal of BaTiO_3 (of dimensions $5 \times 5 \times 5.9$ mm³) at an angle of 42° with respect to the crystal normal. This reference beam had a mea-

sured intensity I_R of 2.4 mW. The beam reflected by BS, the signal beam, traversed a variable neutral density filter VF, and was incident on various transparencies placed at the object plane position shown. The transform lens L, of focal length 10 cm, was adjusted such that the resultant Fourier transform achieved optimum spatial overlap with the reference beam inside the BaTiO_3 .

To ensure that self-pumping [9] did not readily occur, and also to maximise the available coupling from reference to signal beams, the crystal was oriented such that $\theta_1 = 11^\circ$, $\theta_2 = 32^\circ$, $\theta = 12^\circ$, and $\beta = 11^\circ$. The results of the intensity dependent coupling produced were observed at the image plane either directly, or via a TV camera/monitor combination.

Fig. 2 shows good agreement between measured and theoretical values of gain for the measured range of r when using gaussian beams. It is experimentally difficult, if not impossible however, to map the corresponding values of r for all points in the Fourier transform.

Fig. 4 shows four examples of the results obtained, and illustrates the principle of contrast enhancement, feature extraction, and defect enhancement respectively. Fig. 4(a) shows a letter X of actual dimensions $1.2 \text{ mm} \times 0.6 \text{ mm}$ that was used as an input test transparency; the slide was photographically prepared such that the contrast between the letter and the background was very poor. Fig. 4(a) is the result obtained at the image plane from illuminating the slide with the reference beam blocked. With I_R present, however, fig. 4(b) shows that the spatial frequencies corresponding to the letter X have experienced preferentially higher gain compared to the background illumination present in the relatively higher intensity dc term. The photos 4(a) and 4(b) were taken for equal intensity in the letter X, as determined by feature heights on the scenic display, to ensure results that would bear fair comparison.

Figs. 4(c)–4(f) show results for objects which have features possessing high spatial frequencies but whose contrast is poor. Fig. 4(d) shows the enhanced version of a fringe pattern produced by interference in a thin oil film, compared with fig. 4(c), which is the corresponding unenhanced version. Fig. 4(e) shows dust and defects introduced into a

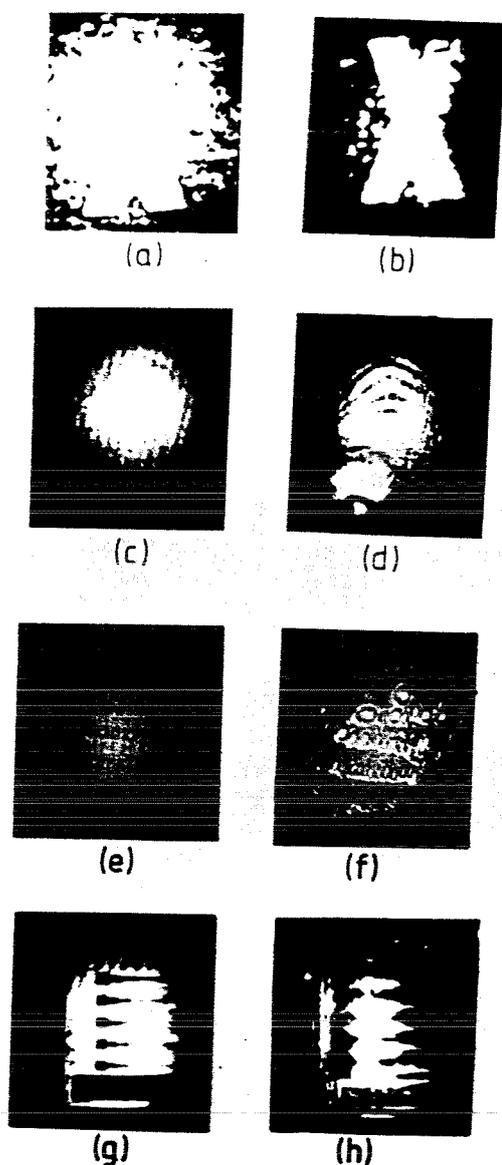


Fig. 4. Results of contrast enhancing, feature extraction, defect enhancement and contrast reversal. Originals are (a), (c), (e) and (f); corresponding enhanced versions are (b), (d), (f) and (h).

smearred oil film whose presence is enhanced in fig. 4(f).

Finally we show an operation of contrast reversal between the original object (part of a periodic test chart) in fig. 4(g) and its contrast reversal replica in

fig. 4(h). This last result is not of particularly good quality but illustrates the possibility discussed by Kolodziejczyk [10] for contrast reversal via spatial filtering, which may be achieved if the dark area in the repeat unit cell is less than half of the total area. For fig. 4(h), the Fourier transform of the periodic object was amplified, and the reference beam subsequently cut. Under normal amplification, only partial contrast inversion was possible.

The loss of resolution evident in fig. 4(h) may be due to one of several reasons. Due to the nature of the two beam coupling process, different portions of the Fourier transform may experience varying interaction lengths within the non spatially uniform reference beam. Also, as I depends on β , θ_1 and θ_2 for each part of the interacting beams, it is to be expected that spatial variations leading to variable resolution will occur.

4. Conclusion

To summarise, we have proposed and demonstrated a technique for controlled modification of selected Fourier components via two beam coupling in photorefractive BaTiO₃. By appropriate choice of operating point on the gain curve, the operations of contrast enhancement, feature extraction defect enhancement and contrast reversal have been demonstrated, and the implications of variable gain rather than selective reduction of an object's Fourier spectrum discussed. We also mention here that in addition to enhancement via coupling, turning the c -axis of the crystal through 180° would result in the more familiar process of low pass filtering, in which high spatial frequencies are coupled out of the signal beam. This is similar, though not equivalent to conventional spatial filtering techniques for two reasons. Firstly the image features associated with the high spatial frequencies are redirected rather than lost, to appear in the reference beam, and secondly the high spatial frequencies are removed according to their intensities. This result is of possible future significance to applications in dynamic noise suppression.

For real time applications BaTiO₃ may well not be the ideal material. Other fast photorefractives such as reduced KNbO₃ or even BSO can be used, in conjunction with moving grating techniques [11] which

increases Γ . There is also the possibility of adding an extra modifying beam for local grating erasure in a manner similar to previous modification work [12,13].

Acknowledgements

The authors are grateful to the Overseas Research Scheme for a studentship for J. Khoury and to the Government of Pakistan for a research studentship for G. Hussain.

References

[1] L.M. Bernardo, H.M. Salgado and O.D.D. Soares, *Optica Acta* 33 (1986) 889.

- [2] J. Feinberg, *Optics Lett.* 5 (1980) 330.
- [3] J.P. Huignard and J.P. Herriau, *Appl. Optics* 17 (1978) 2571.
- [4] N.A. Vainos and R.W. Eason, *Optics Comm.* 59 (1986) 167.
- [5] E. Ochoa, J.W. Goodman and L. Hesselink, *Optics Lett.* 10 (1985) 430.
- [6] Y. Fainman, E. Klancik and S.H. Lee, *Opt. Eng.* 25 (1986) 228.
- [7] N.V. Kukhtarev, V.B. Markov, S.G. Odulov, M.S. Soskin and V.L. Vinetskii, *Ferroelectrics* 22 (1979) 961.
- [8] J. Feinberg, D. Heiman, A.R. Tanguay, Jr. and R.W. Hellwarth, *J. Appl. Phys.* 52 (1980) 1297.
- [9] J. Feinberg, *Optics Lett.* 7 (1982) 486.
- [10] A. Kolodziejczyk, *Optica Acta* 33 (1986) 867.
- [11] J.P. Huignard, H. Rajbenbach, Ph. Refregier and L. Solymar, *Opt. Eng.* 24 (1985) 586.
- [12] Y. Shi, D. Psaltis, A. Marrakchi and A.R. Tanguay, Jr., *Appl. Optics* 22 (1983) 3665.
- [13] M.W. McCall and C.R. Petts, *Optics Comm.* 53 (1985) 7.